Electrogenerated Chemiluminescence of Soliton Waves in Conjugated Polymers

ARTICLE *in* JOURNAL OF THE AMERICAN CHEMICAL SOCIETY · OCTOBER 2009

Impact Factor: 12.11 · DOI: 10.1021/ja9066018 · Source: PubMed

J|A|C|S COMMUNICATIONS

Published on Web 09/22/2009

Electrogenerated Chemiluminescence of Soliton Waves in Conjugated Polymers

Ya-Lan Chang, Rodrigo E. Palacios, Jiun-Tai Chen, Keith J. Stevenson, Song Guo, William M. Lackowski, and Paul F. Barbara*

Department of Chemistry and Biochemistry, Center for Nano- and Molecular Science and Technology, and Center for Electrochemistry, the University of Texas at Austin, Austin, Texas 78712

Received August 4, 2009; E-mail: p.barbara@mail.utexas.edu

We report soliton-like electrogenerated chemiluminescence (ECL) waves from the conjugated polymer poly(9,9-dioctylfluorene-*co*-benzothiadiazole) (F8BT)[1] in spin-coated thin films covering the working electrode of an electrochemical (EC) cell (Figure 1a). Upon EC oxidation, ECL waves are launched <0.1 s after the EC potential E [vs the quasi-reference electrode (QRE)] is stepped from 0 V to >1.5 V (see Figure 1b). The waves are "triggered" by Au nanoparticles (NPs) embedded in the film. This new type of ECL wave differs from previously investigated EC wave phenomena[2] by exhibiting "free waves" that propagate over macroscopic distances with an extraordinarily sharp, self-triggering wave front.

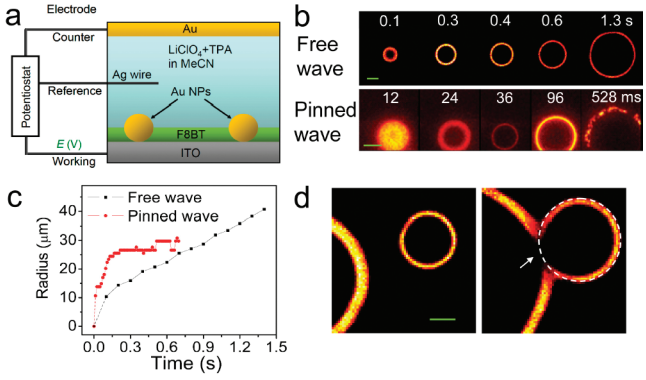

Figure 1. (a) The EC cell includes a silver-wire QRE, a gold planar counter electrode, and a 50 nm conjugated polymer-coated ITO working electrode. (b) Images of free and pinned ECL waves triggered by 250 nm Au NPs with potential steps of 1.5 and 1.8 V, respectively (also see movies S1 and S2 in the Supporting Information). (c) Radius vs time for (b). (d) ECL images at (left) 0.3 and (right) 0.6 s after the potential step of 1.6 V. The integration time was 100 ms (free) and 12 ms (pinned) in (b) and 100 ms in (d). Scale bars are 20 μm.

Figure 1c shows plots of radius versus time for two ECL waves. The more plentiful pinned waves initially expand rapidly from the site of the NP trigger but then in sequence slow down, "break up" into filaments of ECL, and ultimately extinguish, as shown in the lower panel of Figure 1b. In contrast, free waves propagate at approximately constant speed until they collide and merge with other waves (Figure 1d). Thus, colliding ECL waves appear to annihilate each other at their intersections (see the arrow in Figure 1d or movie S3 in the Supporting Information). Once a localized region of the film has been oxidized and the corresponding ECL wave is generated, no further ECL occurs at these domains, as long as the EC potential is held at >1.5 V. Because of the offset of the HOMO energies of indium tin oxide (ITO) and F8BT, the Schottky barrier for charge injection at the ITO−F8BT interface is large enough to severely limit the rate of oxidation in the EC cell in the absence of the formation of an electrochemical double layer. Thus, it is not surprising that the prompt appearance of ECL waves after the application of an EC potential step requires that the polymer film film is locally bridged by either (1) an electrolyte solution leak, e.g., a physical scratch, or (2) an electrical "short", e.g., a Au post prepared by lithography (data not shown), either of which allows for the formation of the local electrochemical double layer. It has not been established whether the Au NPs function as solution leaks or direct electrical connections through the film. Indeed, insulating SiO_2 NPs are also observed to trigger ECL waves (data not shown), so both mechanisms may be operating for Au NPs.

The ECL is generated during EC oxidation by the exothermic charge recombination of polymer polarons P^+ with EC-generated TPA$^\bullet$ radicals via a multistep mechanism.[3−5] The TPA$^\bullet$ radicals are generated by deprotonation of the EC-oxidized form of the reagent, tri-*n*-propylamine (TPA-H), which was included in the acetonitrile/$LiClO_4$ electrolyte solution to promote ECL.[3,4] In Figure 2a−c, ECL free waves are launched by a square-shaped scratch instead of an embedded NP. Both ingoing and outgoing ECL waves are launched simultaneously, demonstrating that the ECL waves move away from their trigger in both directions. For a film with a shallow scratch (Figure 2d), irregular patterns of ECL rather than a free wave are observed.

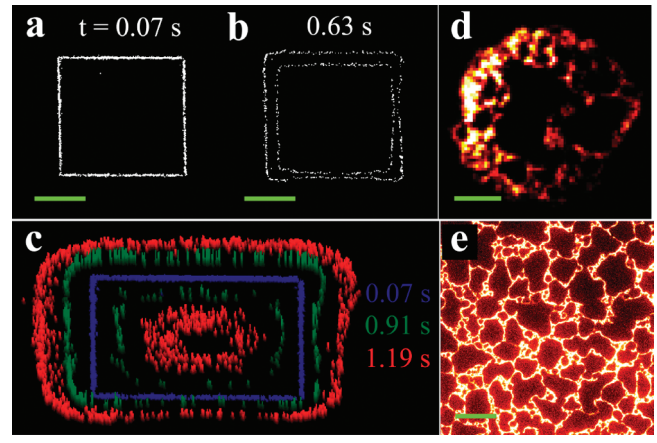

Figure 2. Multiple ECL waves and alternative ECL patterns. (a−c) ECL waves from a ~250 nm film with a square-shaped scratch (90 μm × 90 μm, ~100 nm wide) drawn by an AFM tip (see movie S4), at an applied potential of 1.6 V: (a) ECL image at t = 0.07 s; (b) ECL image at t = 0.63 s; (c) images of a 3D projection (side view) of three ECL images superimposed to show the propagation of ECL waves along both directions of the square scratch. Blue, green, and red lines represent the ECL signals recorded at 0.07, 0.91, and 1.19 s, respectively, after the application of 1.6 V. (d) ECL image of a ~50 nm F8BT film with a shallow scratch (~1 μm in size at the image center) made by pressing an AFM tip into the film, acquired at 7.1 s after the application of 1.8 V. (e) ECL image of a thin F8BT film (~15 nm) during a potential step of 1.8 V. The integration time was (a−c) 70 and (d, e) 100 ms. All scale bars are 40 μm.

10.1021/ja9066018 CCC: $40.75

Similarly, a dense array of triggering leaks for ultrathin films (~15 nm) generates dendritic ECL filaments throughout the film as a result of drying cracks (see Figure 2e). Photoluminescence imaging of P^+ quenching (Figure S1 in the Supporting Information) offers additional evidence that the ECL wave is due to oxidation.

The observation in Figure 1c that the radius of a free wave grows at an approximately constant speed (after the initial rapid growth period) demonstrates that P^+ creation must occur near the wave front rather than at the initial triggering site, suggesting a propagation model in which interface across the wave front between a solvent-swollen, rapidly oxidizing region and a pristine dry region is the major site for P^+ creation. The extremely narrow width of the leading edge of the ECL wave along the direction of propagation is evidence of the nonlinear (thresholdlike) nature of the ECL oxidation kinetics underling this phenomenon. The sharpness of the trailing edge of the ECL wave is probably due, however, to a different phenomenon, i.e., ECL quenching by the buildup of excess P^+ and ultimately by oxidation-induced permanent damage of F8BT, both of which have been described in our previous report on ECL from F8BT NPs.[4] At early times, the shape of the ECL wave front mimics the shape of trigger (scratch or NP), but it tends to become circular at longer times regardless of the original shape of the trigger.

The time dependence of the size of the ECL waves offers additional insights into the sequence of events in the propagation mechanism of the ECL wave front (Figure 1b). NP-triggered waves are particularly well-defined, and since they are nearly perfect circles, the radius can be used as measure of the wave size. As shown in Figure 1c, the slope of the radius-versus-time graph is not constant. For both pinned and free waves, the initial ECL shape is actually a filled circle, or disk, with a radius of ~10 μm rather than a ring at the earliest times we can observe (i.e., 12 ms). This implies that an initial wave speed (e.g., ~800 μm/s, dotted lines in Figure 1c) is orders of the magnitude larger than the terminal (steady-state) speed of the free wave (i.e., 20 μm/s). It is likely that the initial rapid growth of the ECL disk is due to P^+ transport in contact with the electrolyte at the upper surface of the film emanating from the NP−F8BT interface. This mode of hole transport at the electrolyte−polymer film interface should be distinguished from the much slower ion-transport/polymer-swelling mechanism that we propose below for the ring-shaped growth of free and pinned waves. (EC-induced swelling[6] is, furthermore, directly observed by AFM, as shown in Figure S2.)

We hypothesize that propagation of the ECL wave to a fresh region of the polymer film corresponds to physically and chemically switching the fresh region from a dry semiconducting polymer to a swollen (or wet) oxidized polymer that contains charge-compensating anions from the electrolyte. The "switching process" of a fresh region should itself be driven by coupled P^+/electrolyte-anion transport from the adjacent already-switched region. This hypothesis is consistent with the observation that the ECL wave speed increases rapidly with the magnitude of the applied potential because of the increased rate of EC oxidation. The mechanism is also supported by an observed correlation between the curves of EC current versus time and ECL intensity versus time. The EC current increases when the ECL wave begins to propagate because of oxidization of F8BT. If the propagation and growth of a circular ECL wave due to a small scratch is interrupted by returning the potential to 0 V and then a second potential pulse is applied after holding the potential at 0 V for 4 s, a new circular ECL wave is triggered at the original scratch (Figure S3). We note that the second wave actually propagates at a greater speed than the first wave, probably because of the residual solvent in the film. Also, the tendency for circular wave formation is consistent with the isotropic nature of the putative wave front propagation mechanism.

We propose that free ECL waves are produced by a mechanism with the following sequence of kinetically coupled processes: (i) Oxidation in a well-formed EC double layer at the wave front creates positive carriers (P^+) on the top surface of the "dry" film (in contact with the electrolyte solution) ahead of the ECL wave front. (ii) These carriers at the leading edge of the wave "drag" charge-compensating anions and solvent into the polymer film, thereby inducing a phase-transition-like swelling of the partially oxidized polymer ahead of the ECL wave front. (iii) Finally, the swelling transition further enhances transport of solvent molecules and anions into the film, allowing the well-established EC double layer to move forward with the corresponding propagation of the wave.

The soliton EC wave mechanism, which is based on lateral wave propagation, anion-gated EC, and critical polymer swelling transitions, is very different from previously hypothesized mechanisms for the oxidation of semiconducting polymer films.[3,7,8] The proposed soliton EC wave mechanism, furthermore, has important implications for the design and operation of such devices as electrochemical (EC) light-emitting diodes,[9,10] chemically sensitive field-effect transistors (Chem-FETs),[11] electrochromic window coatings,[12] and certain types of solar cells. The results of this work also offer new insights into the well-known break-in phenomena in EC.

Acknowledgment. This work was supported by the National Science Foundation and the Welch Foundation.

Supporting Information Available: Details on materials, experimental procedures, reaction schemes, ECL movies (AVI), and additional supporting data. This material is available free of charge via the Internet at http://pubs.acs.org.

References

(1) Morteani, A. C.; Sreearunothai, P.; Herz, L. M.; Friend, R. H.; Silva, C. *Phys. Rev. Lett.* **2004**, *92*, 247402.
(2) Krischer, K.; Mazouz, N.; Grauel, P. *Angew. Chem., Int. Ed.* **2001**, *40*, 851.
(3) Richter, M. M.; Fan, F. R. F.; Klavetter, F.; Heeger, A. J.; Bard, A. J. *Chem. Phys. Lett.* **1994**, *226*, 115.
(4) Chang, Y. L.; Palacios, R. E.; Fan, F. R. F.; Bard, A. J.; Barbara, P. F. *J. Am. Chem. Soc.* **2008**, *130*, 8906.
(5) Bard, A. J. *Electrogenerated Chemiluminescence*; Marcel Dekker: New York, 2004.
(6) Montilla, F.; Mallavia, R. *J. Phys. Chem. B* **2006**, *110*, 25791.
(7) Dini, D.; Martin, R. E.; Holmes, A. B. *Adv. Funct. Mater.* **2002**, *12*, 299.
(8) Janakiraman, U.; Doblhofer, K.; Fischmeister, C.; Holmes, A. B. *J. Phys. Chem. B* **2004**, *108*, 14368.
(9) Armstrong, N. R.; Wightman, R. M.; Gross, E. M. *Annu. Rev. Phys. Chem.* **2001**, *52*, 391.
(10) Pei, Q.; Heeger, A. J. *Nat. Mater.* **2008**, *7*, 167.
(11) Wang, L.; Fine, D.; Sharma, D.; Torsi, L.; Dodabalapur, A. *Anal. Bioanal. Chem.* **2006**, *384*, 310.
(12) Heuer, H. W.; Wehrmann, R.; Kirchmeyer, S. *Adv. Funct. Mater.* **2002**, *12*, 89.

JA9066018